

Supplementary Materials for

Introducing thermo-mechanochemistry of lignin enabled high-quality low-cost carbon fiber

Yixin Luo¹, Moham Ed Abdur Razzaq¹, Wangda Qu¹, Abdulrahman A. B. A. Mohammed¹,
Alvina Aui¹, Hamidreza Zobeiri¹, Mark Mba Wright¹, Xinwei Wang¹, Xianglan Bai^{1,*}

¹Department of Mechanical Engineering, Iowa State University, Ames, Iowa 50011 USA

*Corresponding author. Email: bxl9801@iastate.edu.

This file includes the following:

Supplementary Text
Tables S1 to S2
Figs. S1 to S7
Supplemental References 1-2

Supplementary text

Analysis of CF Raman results

For calculating the I_D/I_G ratio of CFs, the broad D and G bands in the Raman spectra shown in Fig. 4b & 4c of the main text were deconvoluted into five bands using the Gaussian curve fitting. D_1 peak at 1360cm^{-1} and the D_2 peak at 1620cm^{-1} are disordered carbon in hexagonal carbon layers or at the edges of crystallites. D_3 (1500 cm^{-1}) between D_1 and G (1580 cm^{-1}) and D_4 (1200 cm^{-1}) at the left shoulder of the broad D band is derived from sp^2 -boned amorphous carbon. The peak area sum of D_1 and D_2 divided by the peak area of G was used to calculate the I_D/I_G ratio, representing the disordered sp^2 attached to graphite structures. A lower I_D/I_G ratio represents a higher ordering and reduced structural defect.

Analysis of XRD results:

Before calculating crystalline parameters, Gaussian curve fitting was performed on the broad first band to deconvolute the 002 and γ bands. The Bragg and Scherrer formula was used to calculate crystalline parameters, including interlayer spacing (d_{002}), stacking height (L_c), and lateral length (L_a), as shown below:

$$d_{002} = \lambda / 2 \sin \theta$$

$$L = K \lambda / \beta \cos \theta$$

where θ is the Bragg angle of the corresponding peak. λ is the wavelength of the X-ray. The constant K is 0.89 for the (002) band and 1.84 for (100) . β is the full width at half maximum intensity (FWHM) of the (002) peak and (100) peak. θ is the scattering angle of the corresponding peak. The (002) band measured from the parallel scan was used to calculate L_c , and the (100) band measured from the perpendicular scan was used to calculate L_a .

Analysis of SXAS results

The SAXS results (**Fig. S9**) were used to calculate average pore diameters of CF based on a modified form of the Kalliat model¹ for SXAS measurement by McDonald et al.² shown below:

$$I(q) = \rho^2 I_{OK} \left[\frac{A}{q^n} + \frac{C_{mi}}{(1 + b^2 q^2)^2} \right] + bkg$$

$$\text{the } R = \sqrt{10b}$$

where $I(q)$ is the scattering intensity of the fibers, ρ is the electronic density of graphite. I_{OK} is a parameter associated with the sample mass, the cross-section area of the sample, and the area of the X-ray beam penetrating the sample. q is the wave vector, and A is proportional to the surface area of pores. C_{mi} is proportional to the volume of pores, and b is the Debye autocorrelation length of the pores. R is the radius of the pores, and bkg is the background. n is set up as 3 in this study (for scattering from rough fractal surfaces). While CFs have a distribution of pore sizes, it has been proven that a single characteristic pore size is enough for a reasonable fit to the data instead of a distribution of pore sizes¹.

Table S1 Lignin characterizations after water purification

	Raw OL	Water washed OL	Raw KL	Water washed KL
M_w (g/mol)	2791	3091	4580	5505
Dispersity	4.39	3.8	4.82	4.53
T_g (°C)	95	74	198	156
T_d (°C)	178	196	269	280
Moisture content (%)	1.2	1.22	2.34	1.25
Ash content (%)	1.4	0.07	2.59	0.55
Fixed carbon (%)	37.4	38.7	38.80	39.2

T_d : temperature corresponding to 5% mass loss.

Table S2. Elemental composition of AF, NSF, and TSF

	C (%)	H (%)	N (%)	S (%)	O (%)
AF	67.403	5.063	0.253	0.044	27.236
NSF	64.890	3.293	0.297	0.078	31.442
TSF	64.990	3.366	0.350	0.051	31.243

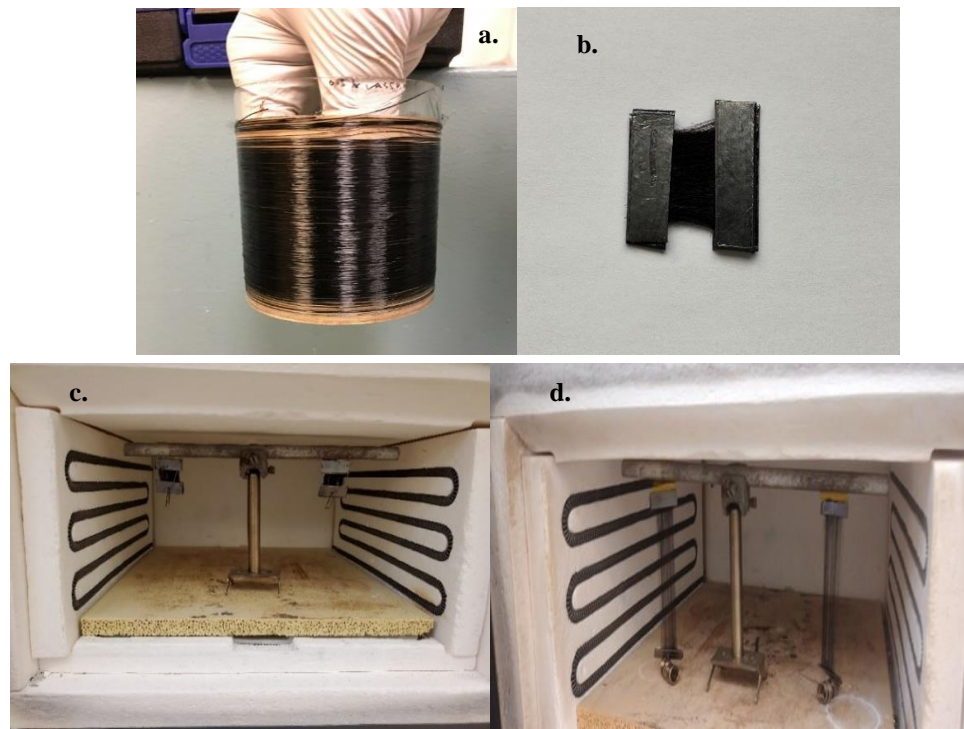


Figure S1. Stabilization of melt-spun fibers. **a.** As-spun fiber (AF) spool; **b.** AF fiber bundles prepared for stabilization; **c & d.** adjustable weights are attached to stretch the spun fibers during stabilization.

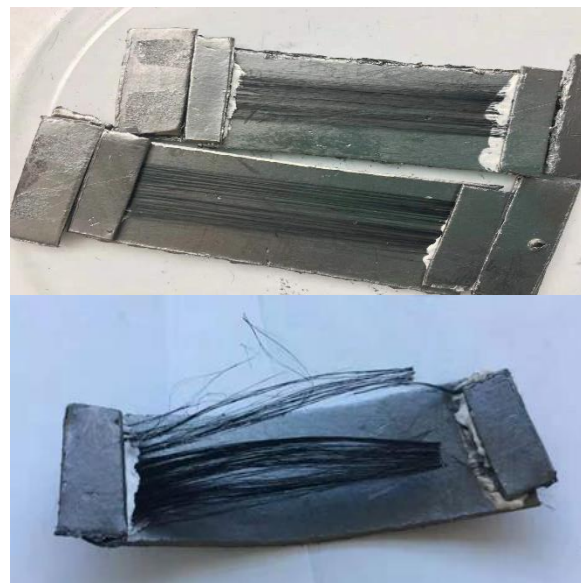


Figure S2. **a.** Stabilized fiber before carbonization; **b.** carbonizing at a constant heating rate of 7°C/min caused excessive fiber shrinkage to bend the graphene sheet and break the fibers.

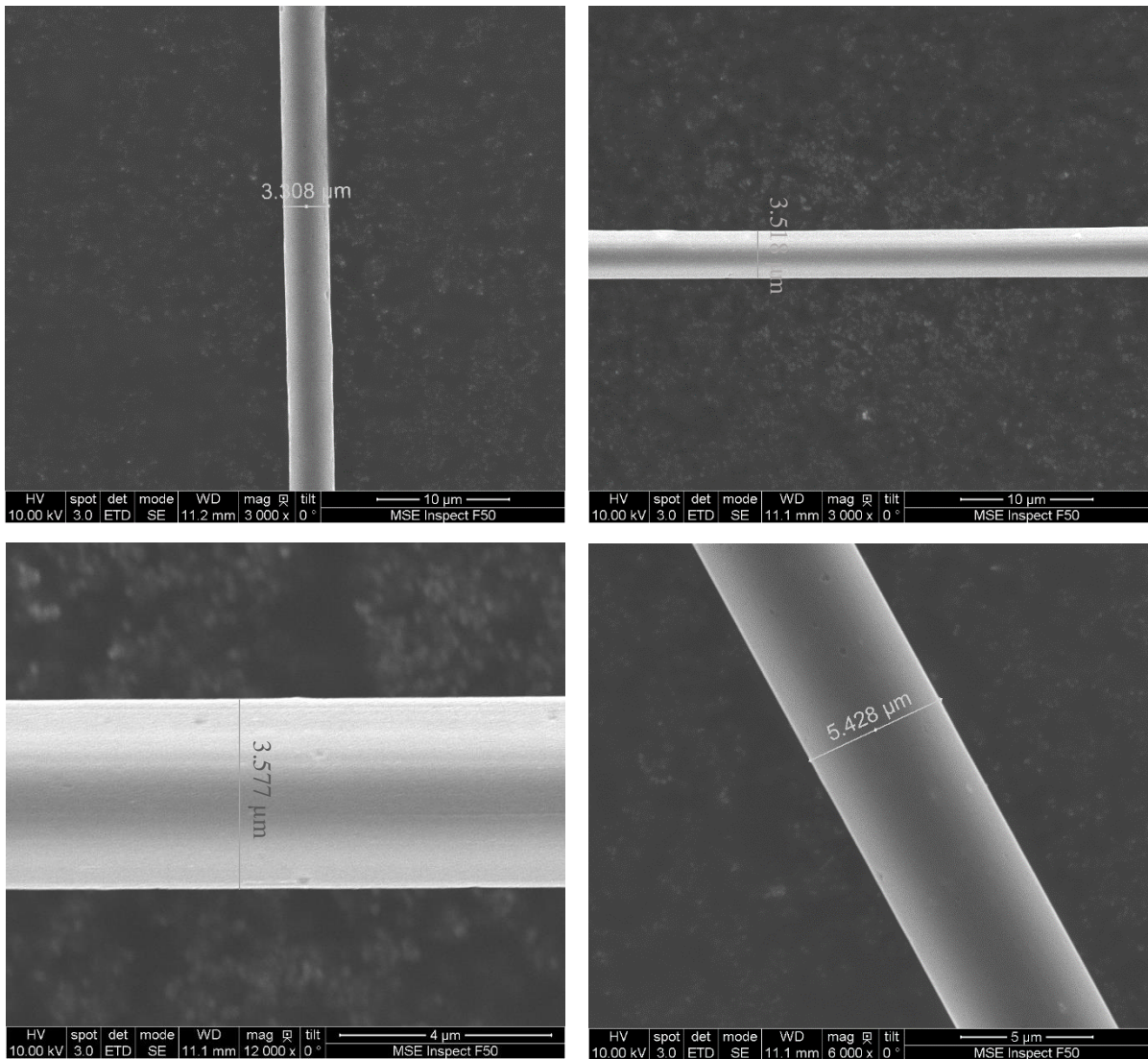


Figure S3. SEM images of representative CFs

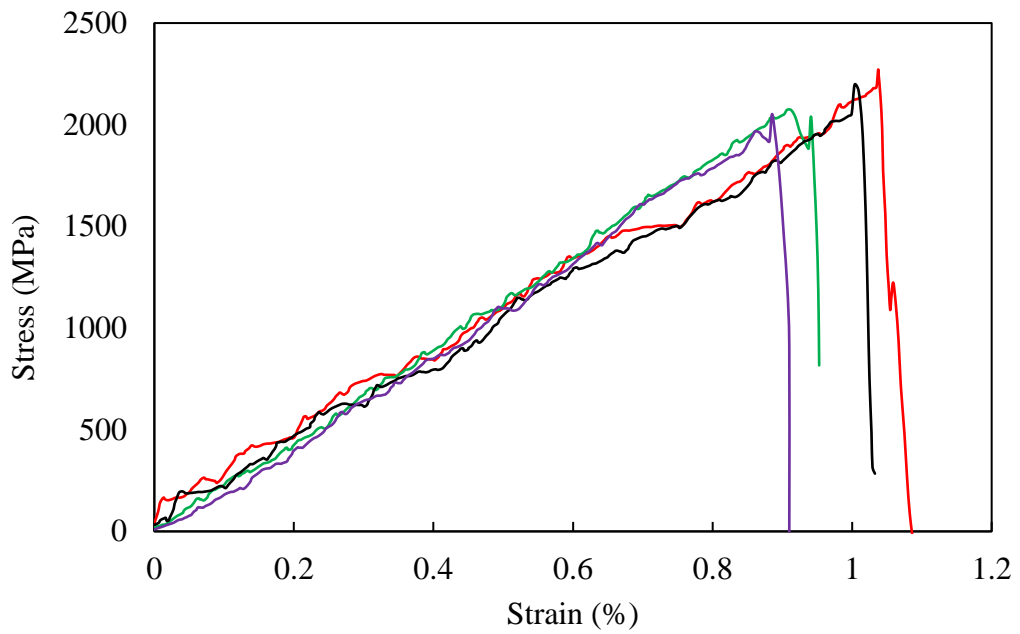


Figure S4. Strain-stress curve

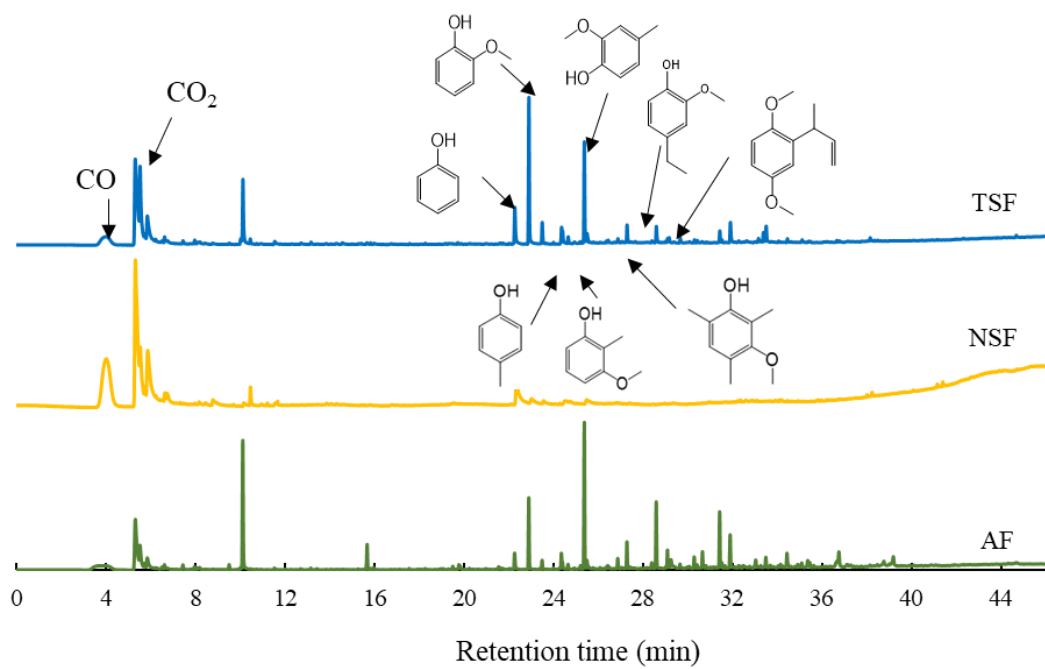


Figure S5. Pyrolysis-GC/MS chromatogram of AF, NSF, and TSF.

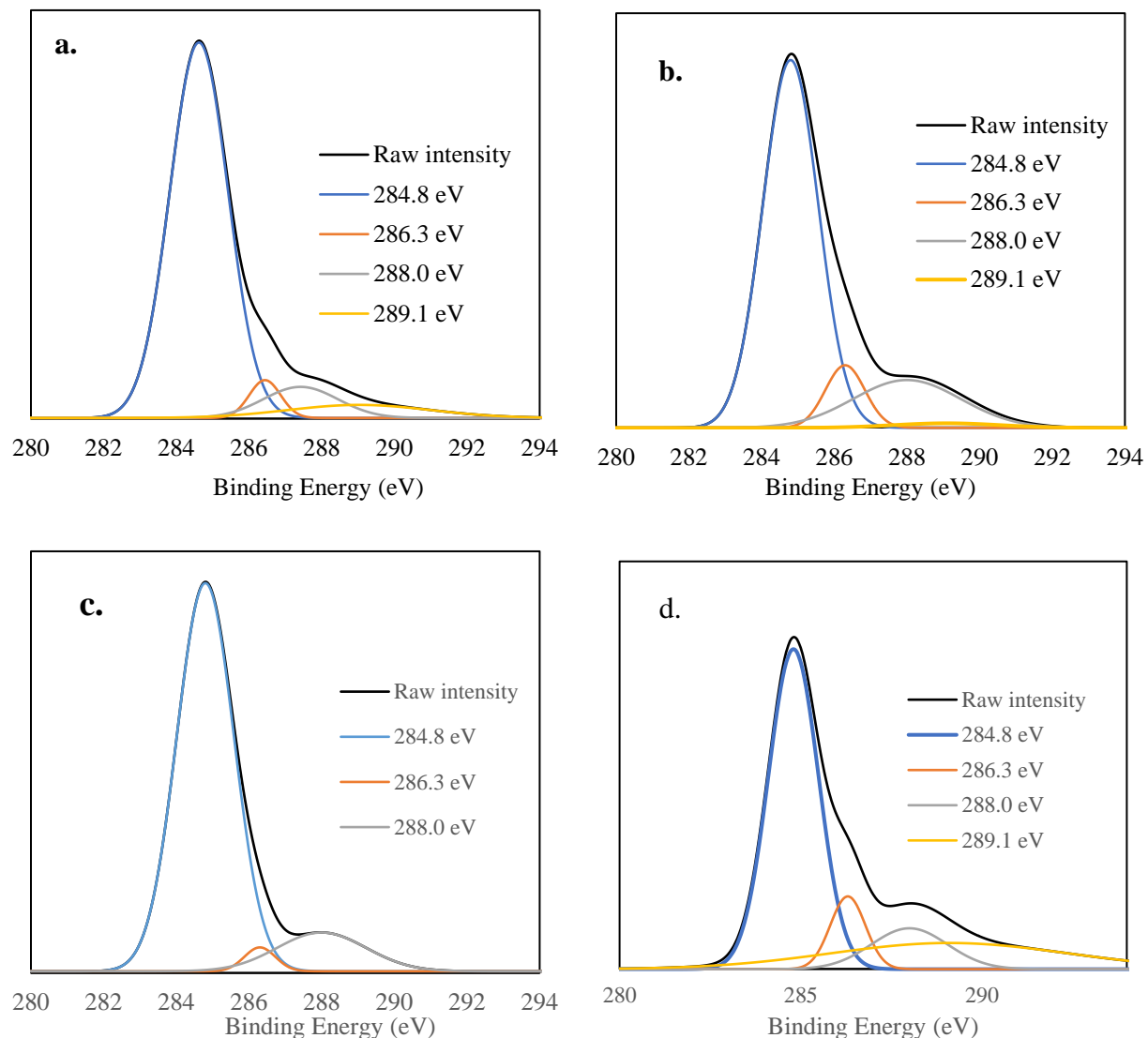
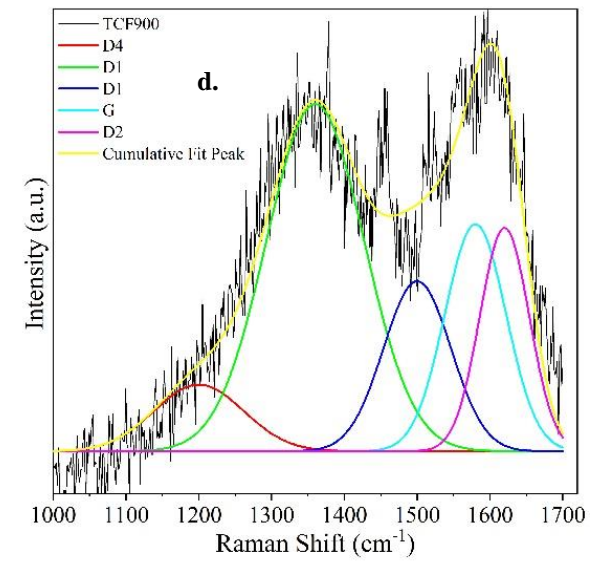
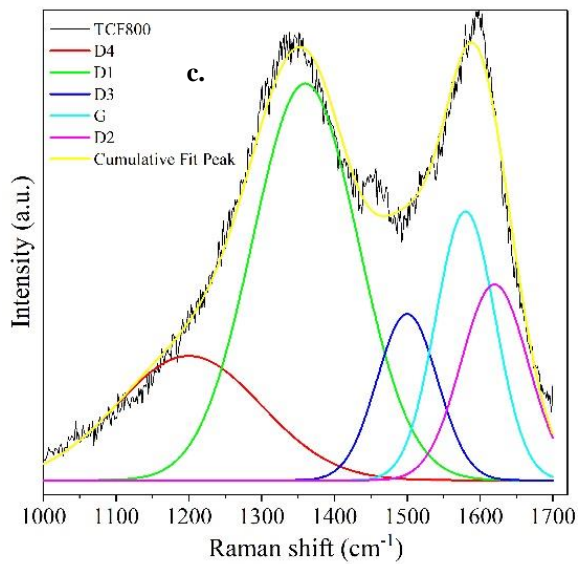
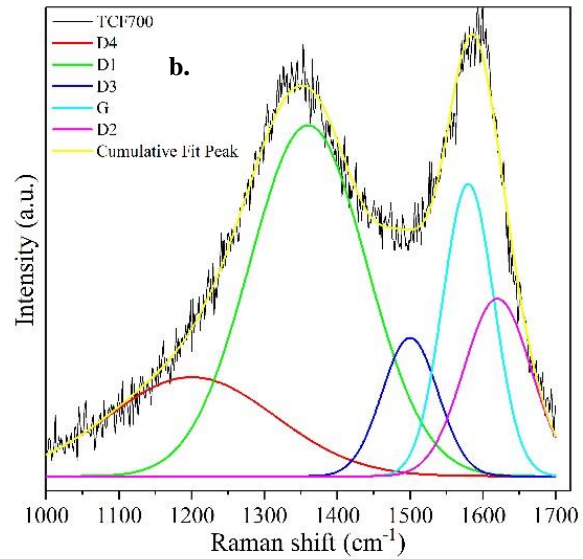
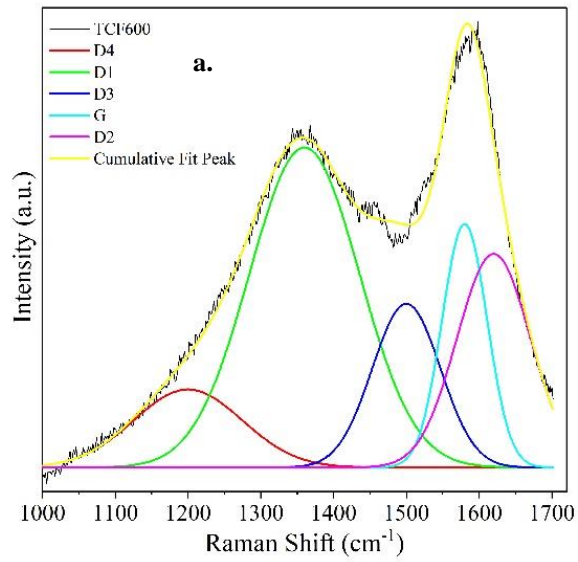
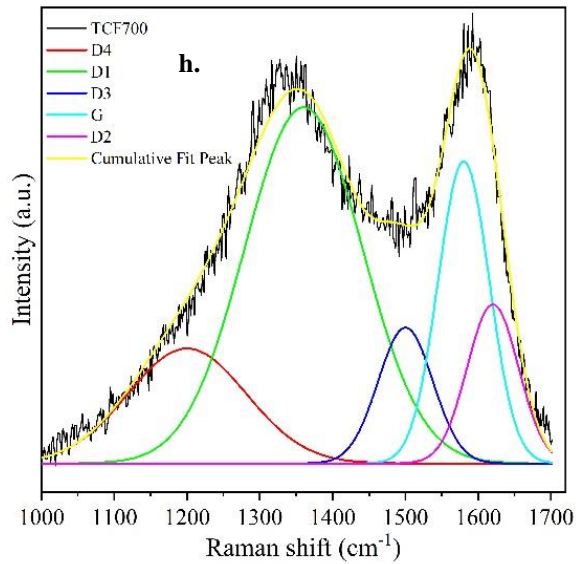
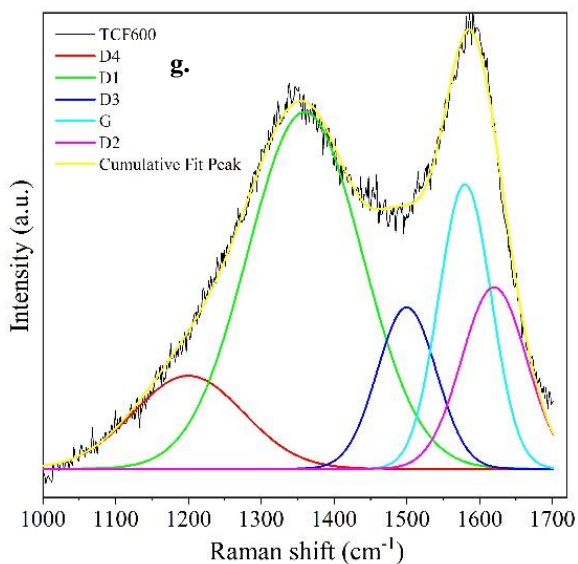
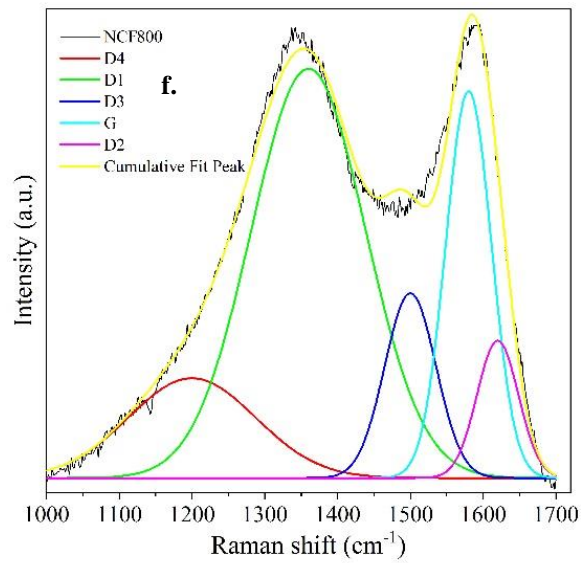
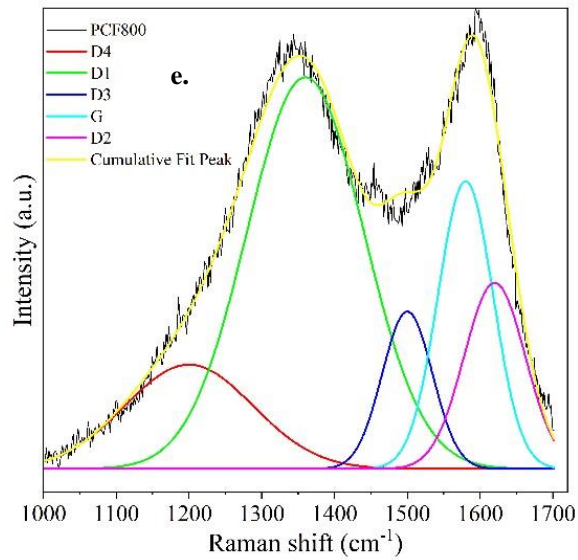


Figure S6. Gaussian fitting of XPS spectra of CFs. **a.** TCF700; **b.** TCF800; **c.** TCF900; **d.** NCF800. 284.8 eV: -C-C-, -C-H-; 286.3 eV: -C-O-; 288.0 eV: -C=O; 289.1 eV: -O-C=O.





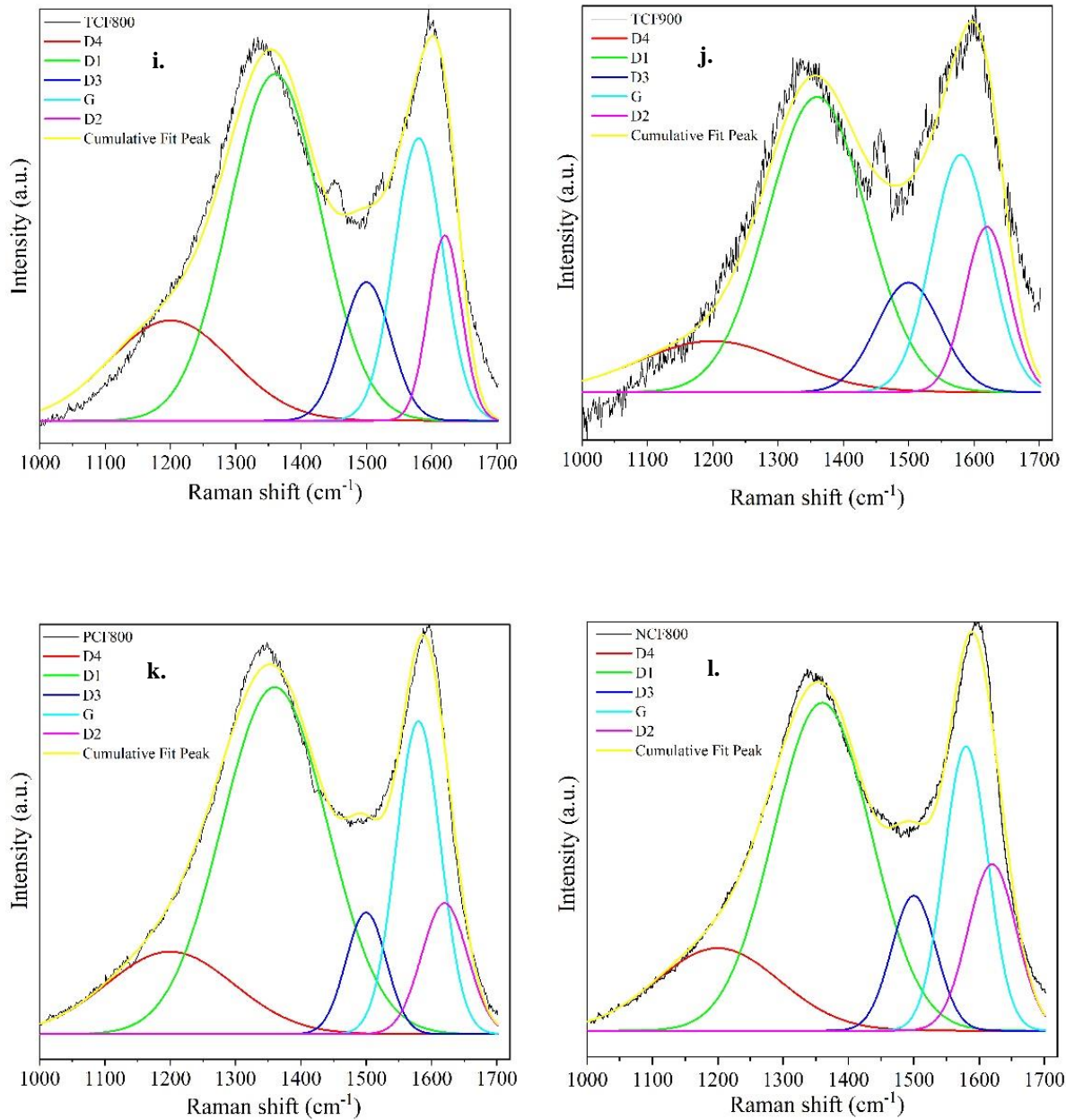
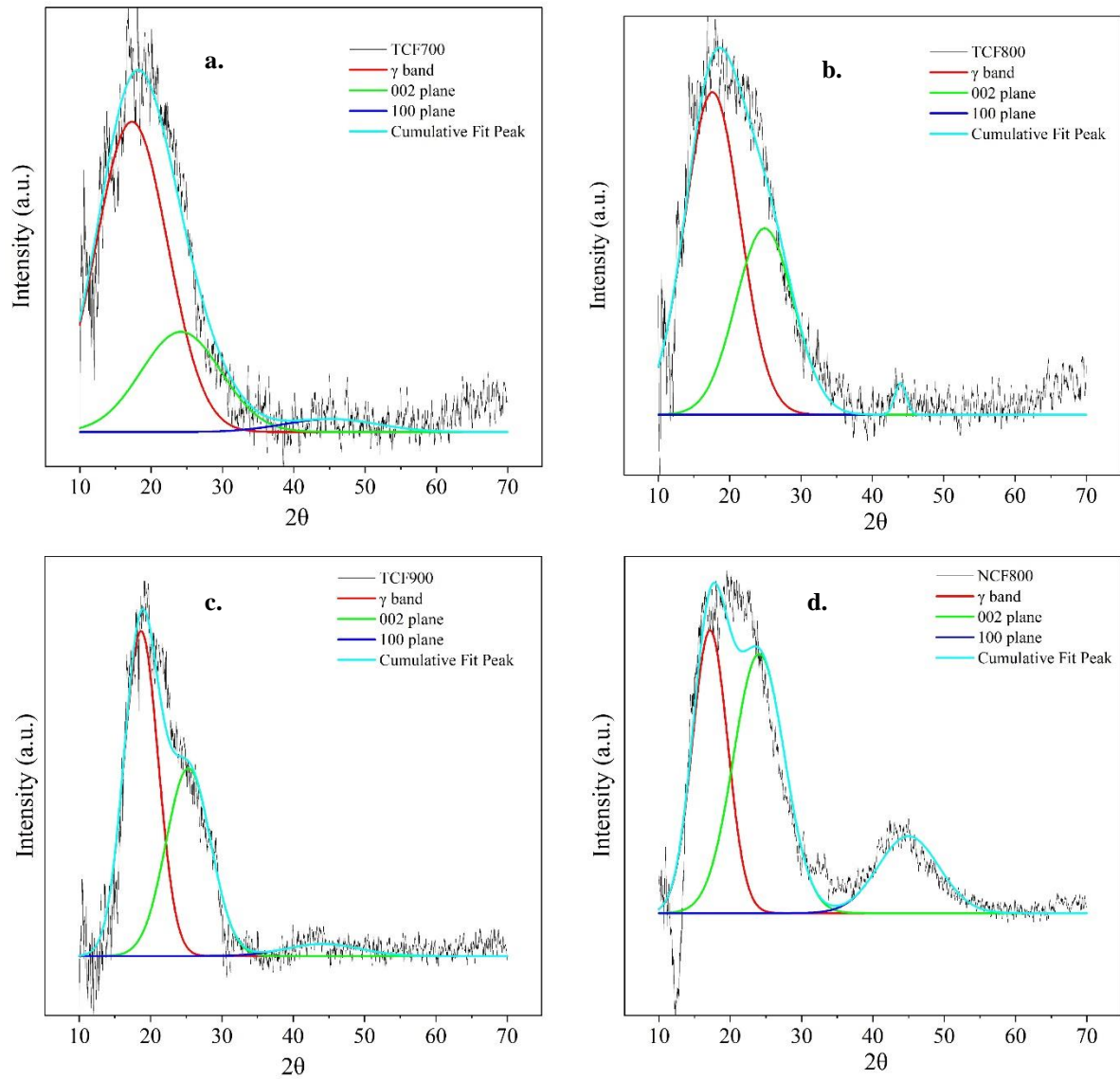


Figure S7. Gaussian fitting of Raman spectra of CFs. For the cross-section view spectra: **a.** TCF600; **b.** TCF700; **c.** TCF800; **d.** TCF900; **e.** PCF800; **f.** NCF800. For the top view spectra: **g.** TCF600; **h.** TCF700; **i.** TCF800; **j.** TCF900; **k.** PCF800; **l.** NCF800.



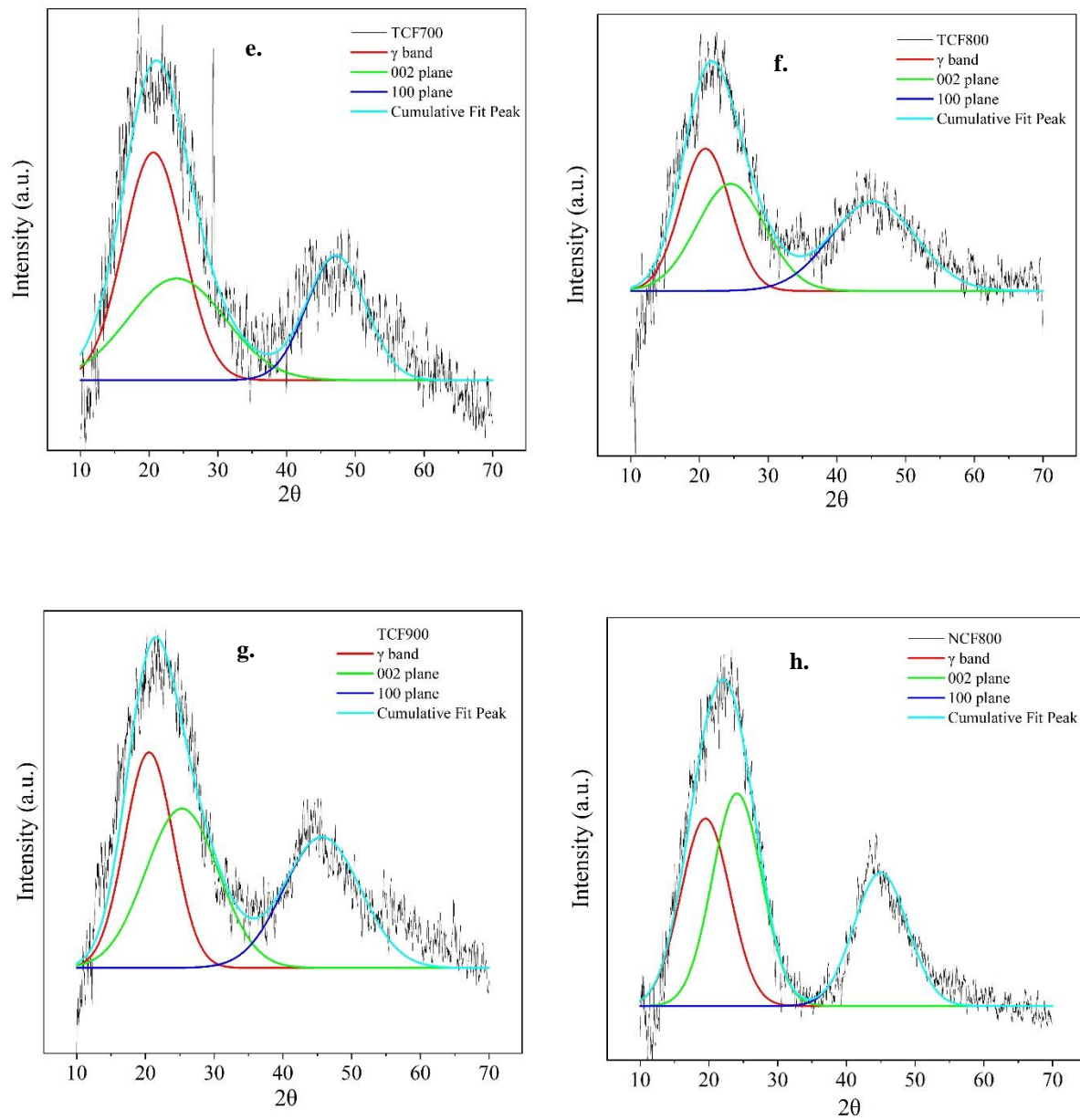


Figure S8. Gaussian fitting of XRD spectra of various CFs. For the parallel scan spectra: **a.** TCF700; **b.** TCF800; **c.** TCF900; **d.** NCF800. For the perpendicular scan spectra: **e.** TCF700; **f.** TCF800; **g.** TCF900; **h.** NCF800.

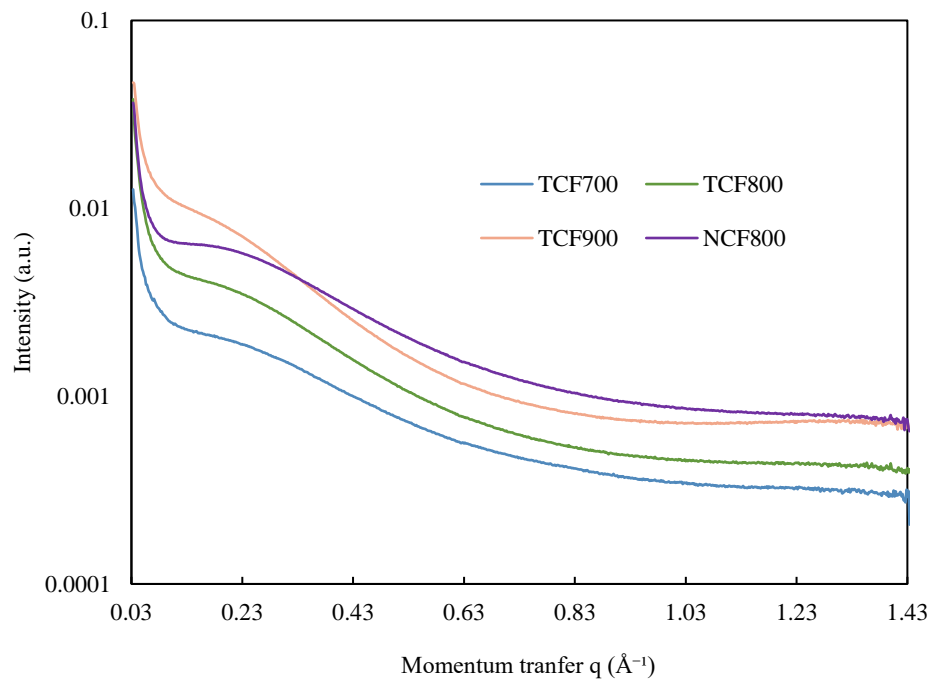


Figure S9. SAXR results of CFs.

Supplemental Material References:

1. M. Kalliat, C. Y. Kwak, and P. W. Schmidt, Small-angle X-ray investigation of the porosity in coals, *New Approaches in Coal Chemistry* Chapter 1, 3-22, ACS Symposium Series 169, ISBN13: 9780841206595 eISBN: 9780841208452, 1981.
2. M. J. McDonald, J. W. H. Smith, and J. R. Dahn, A study of small angle X-ray scattering from impregnated activated carbons, *Carbon* 2014, 68, 452–461, 2014.